Mathematical Modelling and Analysis
Volume 27, Issue 2, 303–321, 2022
https://doi.org/10.3846/mma.2022.14463

Numerical Solutions for 2D Unsteady Laplace-Type Problems of Anisotropic Functionally Graded Materials

Mohammad Ivan Azis

Department of Mathematics, Hasanuddin University
Makassar, Indonesia
E-mail(*corresp.*): ivan@unhas.ac.id

Received February 22, 2021; revised March 18, 2022; accepted March 18, 2022

Abstract. The time-dependent Laplace-type equation of variable coefficients for anisotropic inhomogeneous media is discussed in this paper. Numerical solutions to problems which are governed by the equation are sought by using a combined Laplace transform and boundary element method. The variable coefficients equation is transformed to a constant coefficients equation. The constant coefficients equation after being Laplace transformed is then written in a boundary-only integral equation involving a time-free fundamental solution. The boundary integral equation is therefore employed to find the numerical solutions using a standard boundary element method. Finally the numerical results are inversely transformed numerically using the Stehfest formula to obtain solutions in the time variable. Some problems of anisotropic functionally graded media are considered. The results show that the combined Laplace transform and boundary element method is accurate and easy to implement.

Keywords: anisotropic Laplace-type equation, variable coefficients, Laplace transform, boundary element method.

AMS Subject Classification: 65M38; 35K51; 44A10; 35N10.

1 Introduction

We will consider initial boundary value problems governed by a Laplace-type equation with variable coefficients of the form

$$\frac{\partial}{\partial x_i}\left(\kappa_{ij}\left(\mathbf{x}\right)\frac{\partial\mu\left(\mathbf{x},t\right)}{\partial x_j}\right)=\alpha\left(\mathbf{x},t\right)\frac{\partial\mu\left(\mathbf{x},t\right)}{\partial t}. \tag{1.1}$$

The coefficients $[\kappa_{ij}]$ $(i,j=1,2)$ define a real symmetric positive definite matrix. Also, in (1.1) the summation convention for repeated indices holds. Therefore Equation (1.1) may be written explicitly as

$$\frac{\partial}{\partial x_1}\left(\kappa_{11}\frac{\partial \mu}{\partial x_1}\right)+\frac{\partial}{\partial x_1}\left(\kappa_{12}\frac{\partial \mu}{\partial x_2}\right)+\frac{\partial}{\partial x_2}\left(\kappa_{12}\frac{\partial \mu}{\partial x_1}\right)+\frac{\partial}{\partial x_2}\left(\kappa_{22}\frac{\partial \mu}{\partial x_2}\right)=\alpha\frac{\partial \mu}{\partial t}.$$

Equation (1.1) is usually used to model antiplane strain in elastostatics and plane thermostatic problems (see for examples [18, 24, 26, 31]).

During the last decade functionally graded materials (FGMs) have become an important topic, and numerous studies on them for a variety of applications have been reported. FGMs are materials possessing characteristics which vary (with time and position) according to a mathematical function. Therefore, Equation (1.1) is relevant for FGMs. FGMs are mainly artificial materials which are produced to meet a preset practical performance (see, for example, [1, 2]). This constitutes relevancy of solving Equation (1.1).

Recently a number of authors had been working on the Laplace equation to find its solutions. However the works mainly focus on problems of isotropic homogeneous materials. For example, Guo et al. [11] considered transient heat conduction problems of isotropic and homogeneous media and solved them using a combined Laplace transform and multiple reciprocity boundary face method. In [10] Fu et al. examined a boundary knot method used to find numerical solutions to problems of homogeneous isotropic media governed by a three-dimensional transient heat conduction with a source term. Yang et al. [31] investigated steady nonlinear heat conduction problems of homogeneous isotropic materials and solved them using a radial integration boundary element method. In [9] solutions of a Laplace-type equation in unbounded domains are discussed.

For such kind of materials, the boundary element method (BEM) and other methods had been successfully used to find the numerical solutions of problems associated to them. But this is not the case for inhomogeneous materials, due to the unavailability of fundamental solutions for equations of variable coefficients which govern problems of inhomogeneous media. Some progress of solving problems for inhomogeneous media using various techniques has been done. Timpitak and Pochai [30] investigated finite difference solutions of unsteady diffusion-convection problems for heterogeneous media. Noda et al. [19] studied the analytical solutions to a transient heat conduction equation of variable coefficients with a source term for a functionally graded orthotropic strip (FGOS). In this study, the inhomogeneity of the FGOS is simplified to be functionally graded in the x variable only. In [7] Azis and Clements worked on finding numerical solutions to nonlinear transient heat conduction problems for anisotropic quadratically graded materials using a boundary domain element method. The quadratically varying coefficient in the governing equation considered by Azis and Clements [7] can certainly be represented as a sum of constant and variable coefficients. Some later studies on the class of constant-plus-variable coefficients equations had been done a number of authors. Samec and Škerget [25] considered an unsteady diffusive-convective transport equation with variable velocity which is represented as a sum of constant and variable

terms. Ravnik and Škerget in [22] studied steady-state diffusion-convection problems with inhomogeneous isotropic diffusivity, variable velocity and incompressible fluid using a domain boundary integral equation method (DBIEM). In this work both the diffusivity and the velocity take a constant-plus-variable form. Ravnik and Škerget in [23] considered an unsteady state diffusion-convection problems with sources, inhomogeneous isotropic conductivity, variable velocity and incompressible fluid using a DBIEM. In this study both the diffusivity and the velocity are again taken to be of constant-plus-variable form. AL-Bayati and Wrobel [4,5] focused on convection–diffusion–reaction equation of incompressible flow with constant diffusivity and variable velocity taking the form of constant-plus-variable terms. Ravnik and Tibuat [21] also considered an unsteady diffusion-convection equation with variable diffusivity and velocity. The diffusivity is of the constant-plus-variable form. By taking the variable coefficients as a sum of constant and variable coefficients, the derived integral equation will then involve both boundary and domain integrals. The constant coefficient term will contribute boundary integrals as the fundamental solutions are available, and the variable coefficient term will give domain integrals. Reduction to constant coefficients equation is another technique that can be used to transform a variable coefficients equation to a constant coefficients equation. Therefore the technique will preserve the boundary-only integral equation. Recently Azis and co-workers had been working on steady-state problems of anisotropic inhomogeneous media for several types of governing equations, for examples [6, 12, 20] for Helmholtz equation, [8, 16, 29] for the modified Helmholtz equation, [13] for elasticity problems, [15, 17] for the Laplace-type equation. Some other classes of inhomogeneity functions for FGMs that differ from the class of constant-plus-variable coefficients are reported from these papers.

This paper is intended to extend the recently published works in [15,17] for steady anisotropic Laplace-type equation with spatially variable coefficients of the form

$$\frac{\partial}{\partial x_i}\left(\kappa_{ij}\left(\mathbf{x}\right)\frac{\partial\mu\left(\mathbf{x},t\right)}{\partial x_j}\right)=0$$

to unsteady anisotropic Laplace-type equation with spatially variable coefficients of the form (1.1). Sutradhar and co-workers [27,28] had been working on unsteady Laplace problems, but the works considered isotropic media whereas the present work considers the case of anisotropic media and includes the case of isotropic media as a special case. Equation (1.1) will be transformed to a constant coefficient equation from which a boundary integral equation will derived. It is necessary to place some constraint on the class of coefficients κ_{ij} for which the solution obtained is valid. The analysis of this paper is purely formal; the main aim being to construct effective BEM for a class of equations which falls within the type (1.1).

2 The state of problem

Referred to a Cartesian coordinate system Ox_1x_2, solutions $\mu\left(\mathbf{x},t\right)$ and its derivatives to (1.1) are sought which are valid for time interval $t\geq 0$ and in a

region Ω in R^2 with boundary $\partial\Omega$ which consists of a finite number of piecewise smooth closed curves. On $\partial\Omega_1$ the dependent variable $\mu(\mathbf{x},t)$ ($\mathbf{x}=(x_1,x_2)$) is specified and on $\partial\Omega_2$

$$P(\mathbf{x},t)=\kappa_{ij}(\mathbf{x})\frac{\partial\mu(\mathbf{x},t)}{\partial x_i}n_j \tag{2.1}$$

is specified, where $\partial\Omega=\partial\Omega_1\cup\partial\Omega_2$ and $\mathbf{n}=(n_1,n_2)$ denote the outward pointing normal to $\partial\Omega$. The initial condition is taken to be

$$\mu(\mathbf{x},0)=0. \tag{2.2}$$

The method will transform the variable coefficient Equation (1.1) to a constant coefficient equation, and then taking a Laplace transform of the constant coefficient equation to obtain a boundary integral equation in the Laplace transform variable s. The boundary integral equation is then solved using a boundary element method (BEM) to obtain the solution μ and its derivatives with respect to x_i in the domain. The inverse Laplace transform is implemented numerically using the Stehfest formula.

The analysis is specially relevant to an anisotropic medium but it equally applies to isotropic media. For isotropy, the coefficients in (1.1) take the form $\kappa_{11}=\kappa_{22}$ and $\kappa_{12}=0$ and use of these equations in the following analysis immediately yields the corresponding results for an isotropic medium.

3 The integral equation

The coefficients κ_{ij},α are required to take the form

$$\kappa_{ij}(\mathbf{x})=\overline{\kappa}_{ij}g(\mathbf{x}),\quad \alpha(\mathbf{x})=\overline{\alpha}(t)\,g(\mathbf{x}), \tag{3.1}$$

where the $\overline{\kappa}_{ij},\overline{\alpha}$ are constants and g is a differentiable function of $\mathbf{x}$. Use of (3.1) in (1.1) yields

$$\overline{\kappa}_{ij}\frac{\partial}{\partial x_i}\left(g\frac{\partial\mu}{\partial x_j}\right)=\overline{\alpha}g\frac{\partial\mu}{\partial t}. \tag{3.2}$$

Let

$$\mu(\mathbf{x},t)=g^{-1/2}(\mathbf{x})\,\psi(\mathbf{x},t), \tag{3.3}$$

therefore, substitution of (3.1) and (3.3) into (2.1) gives

$$P(\mathbf{x},t)=-P_g(\mathbf{x})\,\psi(\mathbf{x},t)+g^{1/2}(\mathbf{x})\,P_\psi(\mathbf{x},t), \tag{3.4}$$

where

$$P_g(\mathbf{x})=\overline{\kappa}_{ij}\frac{\partial g^{1/2}}{\partial x_j}n_i \qquad P_\psi(\mathbf{x})=\overline{\kappa}_{ij}\frac{\partial\psi}{\partial x_j}n_i.$$

Also, (3.2) may be written in the form

$$\begin{aligned}
\overline{\kappa}_{ij}\frac{\partial}{\partial x_i}\left[g\frac{\partial\left(g^{-1/2}\psi\right)}{\partial x_j}\right] =& \overline{\alpha}g\frac{\partial\left(g^{-1/2}\psi\right)}{\partial t},\\
\overline{\kappa}_{ij}\frac{\partial}{\partial x_i}\left[g\left(g^{-1/2}\frac{\partial\psi}{\partial x_j}+\psi\frac{\partial g^{-1/2}}{\partial x_j}\right)\right] =& \overline{\alpha}g^{1/2}\frac{\partial\psi}{\partial t},\\
\overline{\kappa}_{ij}\frac{\partial}{\partial x_i}\left(g^{1/2}\frac{\partial\psi}{\partial x_j}+g\psi\frac{\partial g^{-1/2}}{\partial x_j}\right) =& \overline{\alpha}g^{1/2}\frac{\partial\psi}{\partial t}.
\end{aligned}$$

Use of the identity

$$\frac{\partial g^{-1/2}}{\partial x_i}=-g^{-1}\frac{\partial g^{1/2}}{\partial x_i}$$

implies

$$\overline{\kappa}_{ij}\frac{\partial}{\partial x_i}\left(g^{1/2}\frac{\partial\psi}{\partial x_j}-\psi\frac{\partial g^{1/2}}{\partial x_j}\right)=\overline{\alpha}g^{1/2}\frac{\partial\psi}{\partial t}.$$

Rearranging and neglecting some zero terms gives

$$g^{1/2}\overline{\kappa}_{ij}\frac{\partial^2\psi}{\partial x_i\partial x_j}-\psi\overline{\kappa}_{ij}\frac{\partial^2 g^{1/2}}{\partial x_i\partial x_j}=\overline{\alpha}g^{1/2}\frac{\partial\psi}{\partial t}.$$

It follows that if g is such that

$$\overline{\kappa}_{ij}\frac{\partial^2 g^{1/2}}{\partial x_i\partial x_j}-\lambda g^{1/2}=0, \tag{3.5}$$

where λ is a constant, then the transformation (3.3) carries the variable coefficients equation (3.2) to the constant coefficients equation

$$\overline{\kappa}_{ij}\frac{\partial^2\psi}{\partial x_i\partial x_j}-\lambda\psi=\overline{\alpha}\frac{\partial\psi}{\partial t}. \tag{3.6}$$

Taking the Laplace transform of (3.3), (3.4), (3.6) and applying the initial condition (2.2) we obtain

$$\psi^*(\mathbf{x},s)=g^{1/2}(\mathbf{x})\,\mu^*(\mathbf{x},s), \tag{3.7}$$

$$P_{\psi^*}(\mathbf{x},s)=\left[P^*(\mathbf{x},s)+P_g(\mathbf{x})\,\psi^*(\mathbf{x},s)\right]g^{-1/2}(\mathbf{x}), \tag{3.8}$$

$$\overline{\kappa}_{ij}\frac{\partial^2\psi^*}{\partial x_i\partial x_j}-\left(\lambda+s\overline{\alpha}^*\right)\psi^*=0, \tag{3.9}$$

where s is the variable of the Laplace-transformed domain.

A boundary integral equation for the solution of (3.9) is given in the form

$$\eta(\mathbf{x}_0)\,\psi^*(\mathbf{x}_0,s)=\int_{\partial\Omega}\left[\Gamma(\mathbf{x},\mathbf{x}_0)\,\psi^*(\mathbf{x},s)-\Phi(\mathbf{x},\mathbf{x}_0)\,P_{\psi^*}(\mathbf{x},s)\right]dS(\mathbf{x}), \tag{3.10}$$

where $\mathbf{x}_0 = (a,b)$, $\eta = 0$ if $(a,b) \notin \Omega \cup \partial\Omega$, $\eta = 1$ if $(a,b) \in \Omega$, $\eta = \frac{1}{2}$ if $(a,b) \in \partial\Omega$ and $\partial\Omega$ has a continuously turning tangent at (a,b). The so called fundamental solution Φ in (3.10) is any solution of the equation

$$\overline{\kappa}_{ij} \frac{\partial^2 \Phi}{\partial x_i \partial x_j} - (\lambda + s\overline{\alpha}^*)\, \Phi = \delta\,(\mathbf{x} - \mathbf{x}_0) \tag{3.11}$$

and the Γ is given by

$$\Gamma\,(\mathbf{x}, \mathbf{x}_0) = \overline{\kappa}_{ij} \frac{\partial \Phi\,(\mathbf{x}, \mathbf{x}_0)}{\partial x_j} n_i,$$

where δ is the Dirac delta function. For two-dimensional problems, three types of fundamental solutions Φ and Γ that can be obtained from (3.11), namely the fundamental solutions for Laplace equation $(\lambda + s\overline{\alpha} = 0)$, for Helmholtz equation $(\lambda + s\overline{\alpha} < 0)$ and for modified Helmholtz equation $(\lambda + s\overline{\alpha} > 0)$, are given respectively by

$$\begin{aligned}
\Phi\,(\mathbf{x}, \mathbf{x}_0) &= \begin{cases} \frac{K}{2\pi} \ln R & \text{if } \lambda + s\overline{\alpha}^* = 0, \\ \frac{\imath K}{4} H_0^{(2)}\,(\omega R) & \text{if } \lambda + s\overline{\alpha}^* < 0, \\ \frac{-K}{2\pi} K_0\,(\omega R) & \text{if } \lambda + s\overline{\alpha}^* > 0, \end{cases} \\
\Gamma\,(\mathbf{x}, \mathbf{x}_0) &= \begin{cases} \frac{K}{2\pi} \frac{1}{R} \overline{\kappa}_{ij} \frac{\partial R}{\partial x_j} n_i & \text{if } \lambda + s\overline{\alpha}^* = 0, \\ \frac{-\imath K \omega}{4} H_1^{(2)}\,(\omega R)\, \overline{\kappa}_{ij} \frac{\partial R}{\partial x_j} n_i & \text{if } \lambda + s\overline{\alpha}^* < 0, \\ \frac{K\omega}{2\pi} K_1\,(\omega R)\, \overline{\kappa}_{ij} \frac{\partial R}{\partial x_j} n_i & \text{if } \lambda + s\overline{\alpha}^* > 0, \end{cases}
\end{aligned} \tag{3.12}$$

where

$$\begin{aligned}
&K = \ddot{\tau}/D, \quad \omega = \sqrt{|\lambda + s\overline{\alpha}^*|/D}, \quad D = \left[\overline{\kappa}_{11} + 2\overline{\kappa}_{12}\dot{\tau} + \overline{\kappa}_{22}\left(\dot{\tau}^2 + \ddot{\tau}^2\right)\right]/2, \\
&R = \sqrt{(\dot{x}_1 - \dot{a})^2 + (\dot{x}_2 - \dot{b})^2}, \quad \dot{x}_1 = x_1 + \dot{\tau} x_2, \\
&\dot{a} = a + \dot{\tau} b, \quad \dot{x}_2 = \ddot{\tau} x_2, \quad \dot{b} = \ddot{\tau} b,
\end{aligned}$$

where $\dot{\tau}$ and $\ddot{\tau}$ are respectively the real and the positive imaginary parts of the complex root τ of the quadratic

$$\overline{\kappa}_{11} + 2\overline{\kappa}_{12}\tau + \overline{\kappa}_{22}\tau^2 = 0$$

and $H_0^{(2)}$, $H_1^{(2)}$ denote the Hankel function of second kind and order zero and order one respectively. K_0, K_1 denote the modified Bessel function of order zero and order one respectively, $\imath$ represents the square root of minus one. The derivatives $\partial R/\partial x_j$ needed for the calculation of the Γ in (3.12) are given by

$$\begin{aligned}
\frac{\partial R}{\partial x_1} &= \frac{1}{R}\,(\dot{x}_1 - \dot{a})\,, \\
\frac{\partial R}{\partial x_2} &= \dot{\tau}\left[\frac{1}{R}\,(\dot{x}_1 - \dot{a})\right] + \ddot{\tau}\left[\frac{1}{R}\left(\dot{x}_2 - \dot{b}\right)\right].
\end{aligned}$$

Use of (3.7) and (3.8) in (3.10) yields

$$\eta g^{1/2} \mu^* = \int_{\partial\Omega} \left[\left(g^{1/2}\Gamma - P_g \Phi\right)\mu^* - \left(g^{-1/2}\Phi\right) P^*\right] dS. \tag{3.13}$$

This equation provides a boundary integral equation for determining μ^* and its derivatives at all points of Ω.

Knowing the solutions $\mu^*(\mathbf{x}, s)$ and its derivatives $\partial\mu^*/\partial x_1$ and $\partial\mu^*/\partial x_2$ which are obtained from (3.13), the numerical Laplace transform inversion technique using the Stehfest formula is then employed to find the values of $\mu(\mathbf{x}, t)$ and its derivatives $\partial\mu/\partial x_1$ and $\partial\mu/\partial x_2$. The Stehfest formula is

$$\begin{aligned}
\mu(\mathbf{x}, t) &\simeq \frac{\ln 2}{t}\sum_{m=1}^{N} V_m \mu^*(\mathbf{x}, s_m),\\
\frac{\partial\mu(\mathbf{x}, t)}{\partial x_1} &\simeq \frac{\ln 2}{t}\sum_{m=1}^{N} V_m \frac{\partial\mu^*(\mathbf{x}, s_m)}{\partial x_1},\\
\frac{\partial\mu(\mathbf{x}, t)}{\partial x_2} &\simeq \frac{\ln 2}{t}\sum_{m=1}^{N} V_m \frac{\partial\mu^*(\mathbf{x}, s_m)}{\partial x_2},
\end{aligned} \tag{3.14}$$

where

$$s_m = \frac{\ln 2}{t} m,\ V_m = (-1)^{\frac{N}{2}+m} \sum_{k=\left[\frac{m+1}{2}\right]}^{\min\left(m, \frac{N}{2}\right)} \frac{k^{N/2}(2k)!}{\left(\frac{N}{2}-k\right)!k!(k-1)!(m-k)!(2k-m)!}.$$

The analysis of the section requires that the coefficients κ_{ij}, α are of the form (3.1) with g satisfying (3.5). This condition on g allows for considerable choice in the coefficients. For example, when $\lambda = 0$, g can assume a number of multiparameter forms with the parameters being employed to fit the coefficients to numerical data for the coefficients. Possible multiparameter forms include

$$g(\mathbf{x}) = (c_0 + c_1x_1 + c_2x_2)^2,\ \ g(\mathbf{x}) = \left[\Re\{c_0 + c_1z + c_2z^2 + \ldots + c_nz^n\}\right]^2,$$

where the $c_k, k = 1, 2, \ldots, n$ are constants, $\Re$ denotes the real part of a complex number and $z = x_1 + \tau x_2$. More generally, the square of the real part of any analytical function of the complex variable z can serve as a possible form for g. For the case when $\lambda \neq 0$ some possible multiparameter forms of g are

$$g(\mathbf{x}) = \left[A\cos(c_0 + c_1x_1 + c_2x_2) + B\sin(c_0 + c_1x_1 + c_2x_2)\right]^2, \overline{\kappa}_{ij}c_ic_j + \lambda = 0,$$
$$g(\mathbf{x}) = \left[A\exp(c_0 + c_1x_1 + c_2x_2)\right]^2, \overline{\kappa}_{ij}c_ic_j - \lambda = 0,$$

where A, B, c_i are real constants.

4 Numerical examples

In order to verify the analysis used in Section 3 to derive the boundary integral Equation (3.13), we will consider several examples as test problems of analytical solutions and problems without simple analytical solutions.

We assume each problem belongs to a system which is valid in given spatial and time domains and governed by Equation (1.1) and satisfying the initial condition (2.2) and some boundary conditions as mentioned in Section

2. The characteristics of the system which are represented by the coefficients $\kappa_{ij}(\mathbf{x}), \alpha(\mathbf{x})$ in Equation (1.1) are assumed to be of the form (3.1) in which $g(\mathbf{x})$ is a quadratic function of the form (3.2). The coefficients $\kappa_{ij}(\mathbf{x}), \alpha(\mathbf{x})$ may represent respectively the diffusivity or conductivity and the change rate of the unknown $\mu(\mathbf{x}, t)$.

A BEM with constant elements is employed to obtain numerical results. The boundary of the domain is discretized into a number of lines (elements). On each element it is assumed that the values of μ and P are constant. The numerical integration on every element is calculated using the 10-point Bode's rule of order $O\left(h^{11}\right)$ where $9h$ equals the length of the element (see [3]). The time interval is chosen to be $0 \leq t \leq 5$. A FORTRAN script is developed to compute the solutions and a specific FORTRAN command is imposed to calculate the elapsed CPU time for obtaining the solutions. A simple script is also embedded to calculate the values of the coefficients $V_m, m = 1, 2, \ldots, N$ for any even number N. Table 1 shows the values of V_m for several values of N.

Table 1. Values of V_m of the Stehfest formula.

V_m	$N = 6$	$N = 8$	$N = 10$	$N = 12$
V_1	1	$-1/3$	$1/12$	$-1/60$
V_2	-49	$145/3$	$-385/12$	$961/60$
V_3	366	-906	1279	-1247
V_4	-858	$16394/3$	$-46871/3$	$82663/3$
V_5	810	$-43130/3$	$505465/6$	$-1579685/6$
V_6	-270	18730	-236957.5	1324138.7
V_7		$-35840/3$	$1127735/3$	$-58375583/15$
V_8		$8960/3$	$-1020215/3$	$21159859/3$
V_9			164062.5	-8005336.5
V_{10}			-32812.5	5552830.5
V_{11}				-2155507.2
V_{12}				359251.2

4.1 Examples with analytical solutions

Other aspects that will be justified are the convergence (as N increases) and time efficiency for obtaining the numerical solutions.

For all problems in this section, the constant anisotropy coefficient $\overline{\kappa}_{ij}$

$$\overline{\kappa}_{ij} = \begin{bmatrix} 1 & 0.1 \\ 0.1 & 0.85 \end{bmatrix}.$$

The boundary conditions are assumed to be (see Figure 1):

$$\begin{array}{ll} P \text{ given on side AB}, & P \text{ given on side BC}, \\ \mu \text{ given on side CD}, & P \text{ given on side DA}. \end{array}$$

A number of 320 elements of equal length, namely 80 elements on each side of the unit square, are used. For each N, numerical solutions for μ and

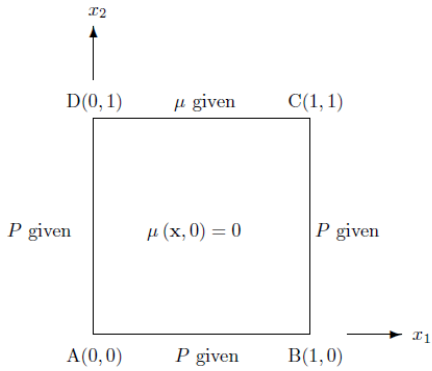

Figure 1. The boundary conditions for the problems in Section 4.1.

the derivatives $\partial\mu/\partial x_1$ and $\partial\mu/\partial x_2$ at 19×19 points inside the space domain, which are

$$(x_1, x_2) = \{0.05, 0.1, 0.15, \ldots, 0.9, 0.95\} \times \{0.05, 0.1, 0.15, \ldots, 0.9, 0.95\}$$

and 11 time-steps, which are $t = 0.0005, 0.5, 1, 1.5, \ldots, 4, 4.5, 5$, are computed. The aggregate relative error E is calculated using the norm

$$E = \left[\frac{\sum_t \sum_{i=1}^{19\times 19} \left(\varsigma_{n,i} - \varsigma_{a,i}\right)^2}{\sum_t \sum_{i=1}^{19\times 19} \varsigma_{a,i}^2} \right]^{\frac{1}{2}},$$

where ς_n and ς_a represent respectively the numerical and analytical solutions μ or the derivatives $\partial\mu/\partial x_1$ and $\partial\mu/\partial x_2$. The elapsed CPU time τ (in seconds) is also computed and the time efficiency number ε for obtaining the numerical solutions of error E is defined as $\varepsilon = E\tau$. This formula explains that the smaller time τ with smaller error E, the more efficient the procedure (smaller ε).

4.1.1 Case 1: trigonometrically graded material

We take

$$g^{1/2}(\mathbf{x}) = \sin\left(1 - 0.15x_1 - 0.3x_2\right).$$

For $g(\mathbf{x})$ to satisfy (3.5) $\lambda = -0.108$. The analytical solution is assumed to take the form (3.3) in which $\psi(\mathbf{x}, t)$ is a separable variables function

$$\psi(\mathbf{x}, t) = h(\mathbf{x}) f(t),$$

where $h(\mathbf{x}), f(t)$ are continuous functions. We choose

$$h(\mathbf{x}) = \exp\left(-0.5 + 0.15x_1 + 0.35x_2\right), \; f(t) = 1 - \exp\left(-1.75t\right).$$

Thus, for $\psi(\mathbf{x})$ to satisfy (3.6),

$$\overline{\alpha}\,(t) = -0.1400714286\,[1 - \exp\,(1.75t)]\,.$$

The analytical solution is then

$$\mu\,(\mathbf{x}, t) = \frac{[1 - \exp\,(-1.75t)]\exp\,(-0.5 + 0.15x_1 + 0.35x_2)}{\sin\,(1 - 0.15x_1 - 0.3x_2)}.$$

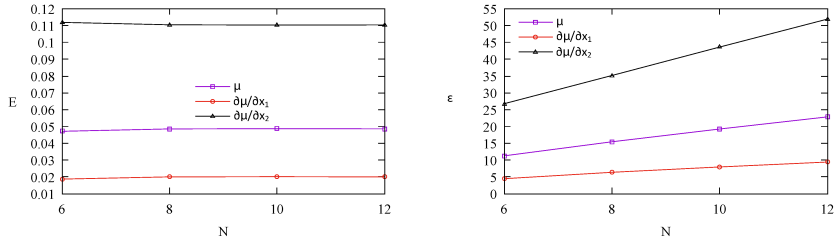

Figure 2. The aggregate relative error E and efficiency number $\varepsilon = \tau E$ for Case 1.

Figure 2, Tables 2 and 3 show the optimal (smallest) error E occurs when $N = 6$ and $N = 10$ for solutions μ, $\partial\mu/\partial x_1$ and $\partial\mu/\partial x_2$, respectively. Meanwhile, the optimal efficiency number ε occurs when $N = 6$ for solutions μ, $\partial\mu/\partial x_1$, $\partial\mu/\partial x_2$. According to Hassanzadeh and Pooladi-Darvish [14], increasing N will increase the accuracy up to a point, and then the accuracy will decline due to round-off errors.

Table 2. The total elapsed CPU time τ, the aggregate relative error E, the efficiency number $\varepsilon = \tau E$ for Case 1.

N		6	8	10	12
τ		239.281	318.375	395.359	470.328
μ	E	0.04715902	0.04857903	0.04870295	0.04860896
	ε	11.284269	15.466349	19.255167	22.862160
$\frac{\partial\mu}{\partial x_1}$	E	0.01874073	0.02004999	0.02015942	0.02006600
	ε	4.484305	6.383415	7.970217	9.437602
$\frac{\partial\mu}{\partial x_2}$	E	0.11193779	0.11047076	0.11034256	0.11041242
	ε	26.784615	35.171129	43.624966	51.930067

In addition, Figure 3 shows the numerical and analytical solutions μ, $\partial\mu/\partial x_1$ and $\partial\mu/\partial x_2$ at $(x_1, x_2) = (0.5, 0.5)$.

4.1.2 Case 2: quadratically graded material

We take

$$g^{1/2}(\mathbf{x}) = 1 - 0.15x_1 - 0.3x_2.$$

Table 3. The optimized value of N for obtaining the numerical solutions $\mu, \partial\mu/\partial x_1, \partial\mu/\partial x_2$ of best error E and efficiency number ε for Case 1.

	μ	$\frac{\partial\mu}{\partial x_1}$	$\frac{\partial\mu}{\partial x_2}$
E	$N=6$	$N=6$	$N=10$
ε	$N=6$	$N=6$	$N=6$

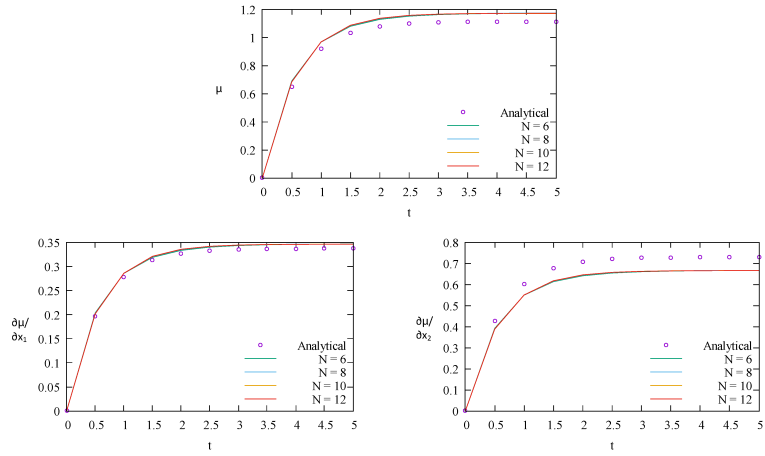

Figure 3. The solutions μ, $\partial\mu/\partial x_1$ and $\partial\mu/\partial x_2$ at $(x_1, x_2) = (0.5, 0.5)$ for Case 1.

For $g(\mathbf{x})$ to satisfy (3.5), $\lambda = 0$. We choose

$$\overline{\alpha}\,(t) = -0.137125t.$$

The analytical solution is

$$\mu\,(\mathbf{x}, t) = \frac{0.2t \sin\,(0.5 - 0.15x_1 - 0.35x_2)}{1 - 0.15x_1 - 0.3x_2}.$$

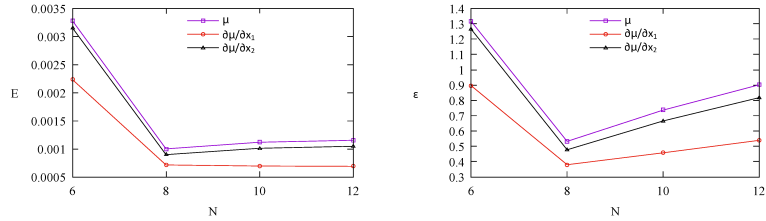

Figure 4. The aggregate relative error E and efficiency number $\varepsilon = \tau E$ for Case 2.

Figure 4, Tables 4 and 5 show that for solutions $\mu, \partial\mu/\partial x_2$ the smallest error E and efficiency number ε are achieved, when $N = 8$, whereas for the solutions $\partial\mu/\partial x_1$ they are reached, when $N = 12$ and $N = 8$ respectively.

Table 4. The total elapsed CPU time τ, the aggregate relative error E, the efficiency number $\varepsilon = \tau E$ for Case 2.

N		6	8	10	12
τ		401.016	532.016	658.406	781.313
μ	E	0.00328027	0.00100093	0.00111835	0.00115346
	ε	1.315440	0.532511	0.736331	0.901213
$\frac{\partial \mu}{\partial x_1}$	E	0.00223307	0.00071443	0.00069532	0.00068988
	ε	0.895495	0.380087	0.457801	0.539008
$\frac{\partial \mu}{\partial x_2}$	E	0.00315254	0.00089786	0.00101098	0.00104635
	ε	1.264219	0.477677	0.665634	0.817526

Table 5. The optimized value of N for obtaining the numerical solutions $\mu, \partial\mu/\partial x_1, \partial\mu/\partial x_2$ of best error E and efficiency number ε for Case 2.

	μ	$\frac{\partial \mu}{\partial x_1}$	$\frac{\partial \mu}{\partial x_2}$
E	$N = 8$	$N = 12$	$N = 8$
ε	$N = 8$	$N = 8$	$N = 8$

Meanwhile, Figure 5 shows the numerical and analytical solutions μ, $\partial\mu/\partial x_1$ and $\partial\mu/\partial x_2$ at $(x_1, x_2) = (0.5, 0.5)$.

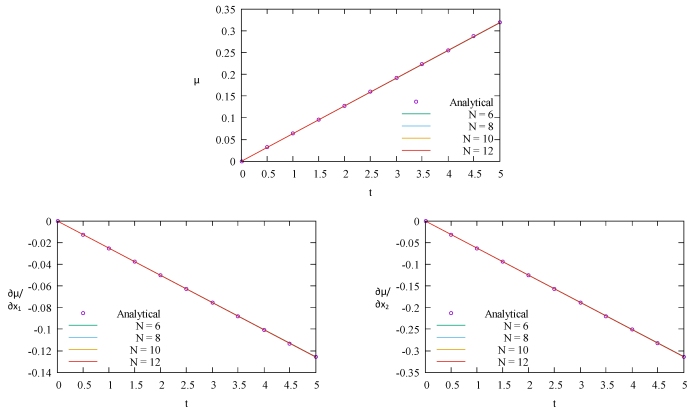

Figure 5. The solutions μ, $\partial\mu/\partial x_1$ and $\partial\mu/\partial x_2$ at $(x_1, x_2) = (0.5, 0.5)$ for Case 2.

4.1.3 Case 3: exponentially graded material

We take

$$g^{1/2}(\mathbf{x}) = \exp\left(-1 + 0.15x_1 + 0.3x_2\right).$$

For $g(\mathbf{x})$ to satisfy (3.5)

$$\lambda = 0.108.$$

We choose

$$\overline{\alpha}(t) = \frac{-0.108t(t-5)}{2t-5}.$$

The analytical solution is

$$\mu(\mathbf{x},t) = \frac{(0.5-0.15x_1-0.35x_2)[0.16t(5-t)]}{\exp(-1+0.15x_1+0.3x_2)}.$$

Figure 6, Tables 6 and 7 show that for solutions $\mu, \partial\mu/\partial x_2$ the smallest error E and efficiency number ε are achieved when $N=10$ and $N=8$, respectively. Whereas for the solution $\partial\mu/\partial x_1$ they are reached when $N=10$.

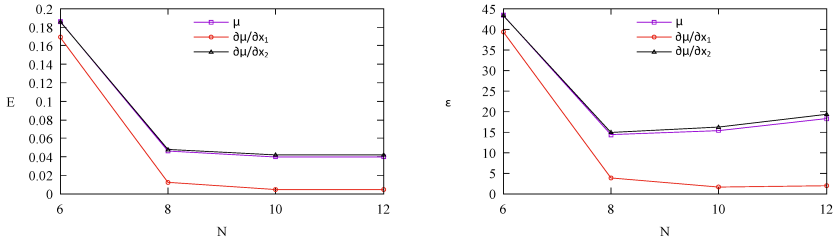

Figure 6. The aggregate relative error E and efficiency number $\varepsilon = \tau E$ for Case 3.

Table 6. The total elapsed CPU time τ, the aggregate relative error E, the efficiency number $\varepsilon = \tau E$ for Case 3.

N		6	8	10	12
τ		233.016	311.281	386.156	458.844
μ	E	0.18639574	0.04624320	0.03977785	0.03987117
	ε	43.433120	14.394641	15.360464	18.294639
$\frac{\partial\mu}{\partial x_1}$	E	0.16917006	0.01238429	0.00423134	0.00425595
	ε	39.419268	3.854996	1.633958	1.952814
$\frac{\partial\mu}{\partial x_2}$	E	0.18613143	0.04793662	0.04203815	0.04212128
	ε	43.371533	14.921772	16.233293	19.327086

Table 7. The optimized value of N for obtaining the numerical solutions $\mu, \partial\mu/\partial x_1, \partial\mu/\partial x_2$ of best error E and efficiency number ε for Case 3.

	μ	$\frac{\partial\mu}{\partial x_1}$	$\frac{\partial\mu}{\partial x_2}$
E	$N=10$	$N=10$	$N=10$
ε	$N=8$	$N=10$	$N=8$

Figure 7 shows the numerical and analytical solutions μ, $\partial\mu/\partial x_1$ and $\partial\mu/\partial x_2$ at $(x_1, x_2) = (0.5, 0.5)$.

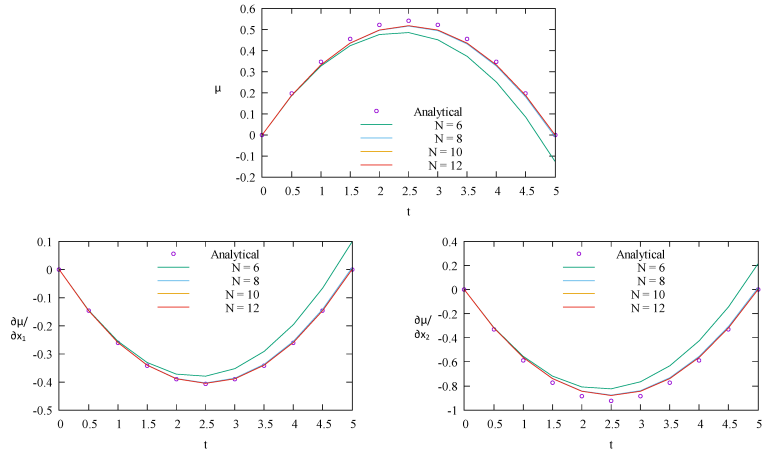

Figure 7. The solutions μ, $\partial\mu/\partial x_1$ and $\partial\mu/\partial x_2$ at $(x_1, x_2) = (0.5, 0.5)$ for Case 3.

4.2 A problem without analytical solution

The aim is to show the effect of inhomogeneity and anisotropy of the considered material on the solution μ.

4.2.1 Problem 2:

The material is supposed to be either quadratically graded or homogeneous with gradation function

$$g^{1/2}(\mathbf{x}) = 1 - 0.15x_1 - 0.3x_2, \qquad g(\mathbf{x}) = 1,$$

respectively, and either anisotropic or isotropic with constant coefficient

$$\overline{\kappa}_{ij} = \begin{bmatrix} 1 & 0.1 \\ 0.1 & 0.85 \end{bmatrix}, \qquad \overline{\kappa}_{ij} = \begin{bmatrix} 1 & 0 \\ 0 & 1 \end{bmatrix},$$

respectively. So that there are four cases regarding the material, namely anisotropic inhomogeneous, anisotropic homogeneous, isotropic inhomogeneous and isotropic homogeneous material.

We set $\overline{\alpha} = 1$ and the boundary conditions are (see Figure 8):

$$\begin{aligned} &P = P(t) \text{ on AB}, \quad P = 0 \text{ on BC}, \\ &\mu = 0 \text{ on CD}, \quad P = 0 \text{ on DA}, \end{aligned}$$

where $P(t)$ takes four cases

$$\begin{aligned} &P(t) = P_1(t) = 1, \;\; P(t) = P_2(t) = 1 - \exp(-1.75t), \\ &P(t) = P_3(t) = t/5, \;\; P(t) = P_4(t) = 0.16t(5 - t). \end{aligned}$$

Therefore, the system is geometrically symmetric about $x_1 = x_2$.

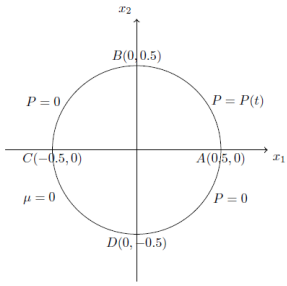

Figure 8. The boundary conditions for Problem 2.

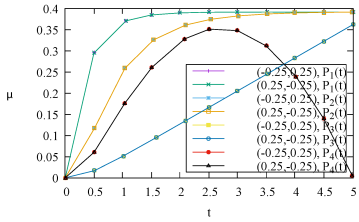

Figure 9. Solution μ at points $(-0.25, 0.25)\,, (0.25, -0.25)$ for Problem 2 of isotropic homogeneous material.

Again, a number of 160 elements of equal length, namely 40 elements on each arc AB, BC, CD and DA of the circle domain, are used. We use $N = 6$ for all cases of this problem. The results are shown in Figures 9, 10 and 11.

Figure 9 depicts solution μ at points $(-0.25, 0.25)\,, (0.25, -0.25)$ when the material under consideration is an isotropic homogeneous material. It can be seen that the values of μ at point $(-0.25, 0.25)$ coincide with those at point $(0.25, -0.25)$. This is to be expected as the system is symmetrical about $x_1 = x_2$ when the material is isotropic homogeneous.

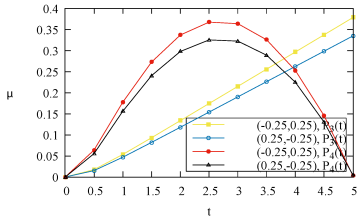

Figure 10. Solution μ at points $(-0.25, 0.25)\,, (0.25, -0.25)$ for Problem 2 of anisotropic homogeneous material.

However, if the material is anisotropic homogeneous the values of μ at point $(-0.25, 0.25)$ do not coincide with those at point $(0.25, -0.25)$. See Figure 10. This means anisotropy gives effect on the values of μ. Similarly, if the material

is isotropic inhomogeneous (see Figure 11) the values of μ at point $(-0.25, 0.25)$ differ from those at point $(0.25, -0.25)$. This indicates that inhomogeneity also gives effect on the values of μ.

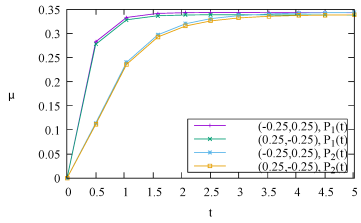

Figure 11. Solution μ at points $(-0.25, 0.25), (0.25, -0.25)$ for Problem 2 of isotropic inhomogeneous material.

In addition, Figures 9, 10 and 11 show that the trends of μ values (as the time t changes) follow the time variation of $P(t)$ except for the form of $P(t) = 1$. This is to be expected as $P(t)$, acting as the boundary condition on side AB, is the only time-dependent quantity for the system. Moreover, as shown in Figures 9 and 11, it is also expected that the values of μ for the cases of $P_1(t) = 1$ and $P_2(t) = 1 - \exp(-1.75t)$ tend to approach same steady state solution as t increases. Both functions $P_1(t)$ and $P_2(t)$ will converge to 1 as t becomes bigger.

5 Conclusions

A combined Laplace transform and BEM has been used to find numerical solutions to initial boundary value problems for anisotropic functionally graded materials which are governed by the Laplace-type equation (1.1). It is easy to implement and accurate. It involves a time variable free fundamental solution and therefore it is quite accurate. Unlikely, the methods with time variable fundamental solution may produce less accurate solutions as the fundamental solution usually has singular time points.

In order to use the boundary integral equation (3.13), the values $\mu(\mathbf{x}, t)$ or $P(\mathbf{x}, t)$ in time variable t of the boundary conditions of the original system as stated in Section 2 have to be Laplace transformed. This means that from the beginning when we set up a problem, we actually put a set of approached boundary conditions. Therefore, it is really important to find a very accurate technique of numerical Laplace transform inversion. Based on the results of Problem 1, the Stehfest formula (3.14) is quite accurate.

The combined method has been implemented to a class of functionally graded materials where the coefficients $\kappa_{ij}(\mathbf{x})$ and $\alpha(\mathbf{x})$ depend on the spatial variable $\mathbf{x}$ only with the same inhomogeneity or gradation function $g(\mathbf{x})$. It will be interesting to extend the study in the future to the case when the coefficients depend on different gradation functions varying also with the time variable t.

Acknowledgements

This work was supported by Universitas Hasanuddin and Kementerian Pendidikan, Kebudayaan, Riset, dan Teknologi Indonesia.

References

[1] H. Abadikhah and P.D. Folkow. Dynamic equations for solid isotropic radially functionally graded circular cylinders. *Composite Structures*, **195**:147–157, 2018. https://doi.org/j.compstruct.2018.03.087.

[2] S. Abotula, A. Kidane, V.B. Chalivendra and A. Shukla. Dynamic curving cracks in functionally graded materials under thermo-mechanical loading. *International Journal of Solids and Structures*, **49**:1637–1655, 2012. https://doi.org/10.1016/j.ijsolstr.2012.03.010.

[3] M. Abramowitz and I.A. Stegun. *Handbook of Mathematical Functions: With Formulas, Graphs and Mathematical Tables*. Dover Publications, Washington, 1972.

[4] S.A. AL-Bayati and L.C. Wrobel. The dual reciprocity boundary element formulation for convection-diffusion-reaction problems with variable velocity field using different radial basis functions. *International Journal of Mechanical Sciences*, **145**:367–377, 2018. https://doi.org/10.1016/j.ijmecsci.2018.07.003.

[5] S.A. AL-Bayati and L.C. Wrobel. A novel dual reciprocity boundary element formulation for two-dimensional transient convection–diffusion–reaction problems with variable velocity. *Engineering Analysis with Boundary Elements*, **94**:60–68, 2018. https://doi.org/10.1016/j.enganabound.2018.06.001.

[6] M.I. Azis. BEM solutions to exponentially variable coefficient Helmholtz equation of anisotropic media. *Journal of Physics: Conference Series*, **1277**:012036, 2019. https://doi.org/10.1088/1742-6596/1277/1/012036.

[7] M.I. Azis and D.L. Clements. Nonlinear transient heat conduction problems for a class of inhomogeneous anisotropic materials by BEM. *Engineering Analysis with Boundary Elements*, **32**:1054–1060, 2008. https://doi.org/10.1016/j.enganabound.2007.04.007.

[8] M.I. Azis, R. Syam and S. Hamzah. BEM solutions to BVPs governed by the anisotropic modified Helmholtz equation for quadratically graded media. *IOP Conference Series: Earth and Environmental Science*, **279**:012010, 2019. https://doi.org/10.1088/1755-1315/279/1/012010.

[9] Y. Chen and Q. Du. Some fast algorithms for exterior anisotropic problems in concave angle domains. *IAENG International Journal of Applied Mathematics*, **50**(4):729–733, 2020.

[10] Z. Fu, J. Shi, W. Chen and L. Yang. Three-dimensional transient heat conduction analysis by boundary knot method. *Mathematics and Computers in Simulation*, **165**:306–317, 2019. https://doi.org/10.1016/j.matcom.2018.11.025.

[11] S. Guo, J. Zhang, G. Li and F. Zhou. Three-dimensional transient heat conduction analysis by Laplace transformation and multiple reciprocity boundary face method. *Engineering Analysis with Boundary Elements*, **37**:15, 2013. https://doi.org/10.1016/j.enganabound.2012.09.001.

[12] S. Hamzah, M.I. Azis and A.K. Amir. Numerical solutions to anisotropic BVPs for quadratically graded media governed by a Helmholtz equation. *IOP Conf. Ser.: Mater. Sci. Eng.*, **619**:012060, 2019. https://doi.org/10.1088/1757-899X/619/1/012060.

[13] S. Hamzah, M.I. Azis, A. Haddade and E. Syamsuddin. On some examples of BEM solution to elasticity problems of isotropic functionally graded materials. *IOP Conf. Ser.: Mater. Sci. Eng.*, **619**:012018, 2019. https://doi.org/10.1088/1757-899X/619/1/012018.

[14] H. Hassanzadeh and H. Pooladi-Darvish. Comparison of different numerical Laplace inversion methods for engineering applications. *Appl. Math. Comput.*, **189**:1966–1981, 2007. https://doi.org/10.1016/j.amc.2006.12.072.

[15] St.N. Jabir, M.I. Azis, Z. Djafar and B. Nurwahyu. BEM solutions to a class of elliptic BVPs for anisotropic trigonometrically graded media. *IOP Conf. Ser.: Mater. Sci. Eng.*, **619**:012059, 2019. https://doi.org/10.1088/1757-899X/619/1/012059.

[16] N. Lanafie, M.I. Azis and Fahruddin. Numerical solutions to BVPs governed by the anisotropic modified Helmholtz equation for trigonometrically graded media. *IOP Conf. Ser.: Mater. Sci. Eng.*, **619**:012058, 2019. https://doi.org/10.1088/1757-899X/619/1/012058.

[17] N. Lanafie, N. Ilyas, M.I. Azis and A.K. Amir. A class of variable coefficient elliptic equations solved using BEM. *IOP Conf. Ser.: Mater. Sci. Eng.*, **619**:012025, 2019. https://doi.org/10.1088/1757-899X/619/1/012025.

[18] Q. Li, S. Chen and X. Luo. Steady heat conduction analyses using an interpolating element-free Galerkin scaled boundary method. *Applied Mathematics and Computation*, **300**:103–115, 2017. https://doi.org/10.1016/j.amc.2016.12.007.

[19] N. Noda, N. Sumi and M. Ohmichi. Analysis of transient plane thermal stresses in functionally graded orthotropic strip. *Journal of Thermal Stresses*, **41**:1225–1243, 2018. https://doi.org/10.1080/01495739.2018.1505445.

[20] B. Nurwahyu, B. Abdullah, A. Massinai and M.I. Azis. Numerical solutions for BVPs governed by a Helmholtz equation of anisotropic FGM. *IOP Conf. Ser.: Earth Environ. Sci.*, **279**:012008, 2019. https://doi.org/10.1088/1755-1315/279/1/012008.

[21] J. Ravnik and J. Tibuat. Fast boundary-domain integral method for unsteady convection-diffusion equation with variable diffusivity using the modified Helmholtz fundamental solution. *Numerical Algorithms*, **82**:1441–1466, 2019. https://doi.org/10.1007/s11075-019-00664-3.

[22] J. Ravnik and L. Škerget. A gradient free integral equation for diffusion–convection equation with variable coefficient and velocity. *Engineering Analysis with Boundary Elements*, **37**:683–690, 2013. https://doi.org/10.1016/j.enganabound.2013.01.012.

[23] J. Ravnik and L. Škerget. Integral equation formulation of an unsteady diffusion–convection equation with variable coefficient and velocity. *Computers and Mathematics with Applications*, **66**:2477–2488, 2014. https://doi.org/10.1016/j.camwa.2013.09.021.

[24] S.Y. Reutskiy. A meshless radial basis function method for 2D steady-state heat conduction problems in anisotropic and inhomogeneous media. *Engineering Analysis with Boundary Elements*, **66**:1–11, 2016. https://doi.org/10.1016/j.enganabound.2016.01.013.

[25] N. Samec and L. Škerget. Integral formulation of a diffusive–convective transport equation for reacting flows. *Engineering Analysis with Boundary Elements*, **28**:1055–1060, 2004. https://doi.org/10.1016/j.enganabound.2004.02.005.

[26] Y.C. Shiah, Y-C. Chaing and T. Matsumoto. Analytical transformation of volume integral for the time-stepping BEM analysis of 2D transient heat conduction in anisotropic media. *Engineering Analysis with Boundary Elements*, **64**:101–110, 2016. https://doi.org/10.1016/j.enganabound.2015.12.008.

[27] A. Sutradhar and G.H. Paulino. The simple boundary element method for transient heat conduction in functionally graded materials. *Computer Methods in Applied Mechanics and Engineering*, **193**:4511–4539, 2004. https://doi.org/10.1016/j.cma.2004.02.018.

[28] A. Sutradhar, G.H. Paulino and L.J. Gray. Transient heat conduction in homogeneous and non-homogeneous materials by the Laplace transform Galerkin boundary element method. *Engineering Analysis with Boundary Elements*, **26**(2):119–132, 2002. https://doi.org/10.1016/S0955-7997(01)00090-X.

[29] R. Syam, Fahruddin, M.I. Azis and A. Hayat. Numerical solutions to anisotropic FGM BVPs governed by the modified Helmholtz type equation. *IOP Conf. Ser.: Mater. Sci. Eng.*, **619**:012061, 2019. https://doi.org/10.1088/1757-899X/619/1/012061.

[30] W. Timpitak and N. Pochai. Numerical simulations to a one-dimensional groundwater pollution measurement model through heterogeneous soil. *IAENG International Journal of Applied Mathematics*, **50**(3):558–565, 2020.

[31] K. Yang, W.Z. Feng, J. Wang and X.W. Gao. RIBEM for 2D and 3D nonlinear heat conduction with temperature dependent conductivity. *Engineering Analysis with Boundary Elements*, **87**:1–8, 2018. https://doi.org/10.1016/j.enganabound.2017.11.001.